# Stochastic analysis of bistability in coherent mixed feedback loops combining transcriptional and posttranscriptional regulations

Mor Nitzan,[1,2] Yishai Shimoni,[1,2,3] Oded Rosolio,[1] Hanah Margalit,[2] and Ofer Biham[1]
[1]*Racah Institute of Physics, Hebrew University, Jerusalem 91904, Israel*
[2]*Department of Microbiology and Molecular Genetics, IMRIC, Faculty of Medicine, Hebrew University, Jerusalem 91120, Israel*
[3]*Center for Computational Biology and Bioinformatics (C2B2), Columbia University, New York, New York 10027, USA*
(Received 29 August 2014; revised manuscript received 5 February 2015; published 15 May 2015)

Mixed feedback loops combining transcriptional and posttranscriptional regulations are common in cellular regulatory networks. They consist of two genes, encoding a transcription factor and a small noncoding RNA (sRNA), which mutually regulate each other's expression. We present a theoretical and numerical study of coherent mixed feedback loops of this type, in which both regulations are negative. Under suitable conditions, these feedback loops are expected to exhibit bistability, namely, two stable states, one dominated by the transcriptional repressor and the other dominated by the sRNA. We use deterministic methods based on rate equation models, in order to identify the range of parameters in which bistability takes place. However, the deterministic models do not account for the finite lifetimes of the bistable states and the spontaneous, fluctuation-driven transitions between them. Therefore, we use stochastic methods to calculate the average lifetimes of the two states. It is found that these lifetimes strongly depend on rate coefficients such as the transcription rates of the transcriptional repressor and the sRNA. In particular, we show that the fraction of time the system spends in the sRNA-dominated state follows a monotonically decreasing sigmoid function of the transcriptional repressor transcription rate. The biological relevance of these results is discussed in the context of such mixed feedback loops in *Escherichia coli*. It is shown that the fluctuation-driven transitions and the dependence of some rate coefficients on the biological conditions enable the cells to switch to the state which is better suited for the existing conditions and to remain in that state as long as these conditions persist.

DOI: 10.1103/PhysRevE.91.052706 PACS number(s): 87.10.Mn, 87.10.Rt, 87.16.A−, 87.16.dj

## I. INTRODUCTION

Recent studies of the interactions between molecules in living cells revealed a complex interplay between regulatory interactions. The regulatory mechanism that was most thoroughly investigated is transcriptional regulation, in which transcription factor (TF) proteins bind to specific promoter sites on the DNA and regulate the transcription of downstream genes. Recently, the significance of posttranscriptional regulation by small noncoding RNA (sRNA) molecules has been recognized, and is now known to play a major role in cellular processes [1–6]. It was suggested that this regulation mechanism would be energetically efficient, since the sRNA molecules are relatively short and are not translated into proteins [5]. More recently, a quantitative analysis has shown that posttranscriptional regulation by sRNA molecules provides fine tuning of the regulation strength [7] and is advantageous when fast responses to external stimuli are needed [4,8,9,10].

Regulatory interactions (such as the ones presented above) can be described by a network in which genes and their products are represented by nodes, while the interactions between them are represented by edges. Analysis of such networks revealed structural modules or motifs, such as the autoregulator and the feedforward loop, which occur statistically significantly more often than randomly expected, and are expected to be of functional importance [11–14]. Some of these motifs include only transcriptional regulation, while others combine different layers of regulation [8,13–16].

An important class of modules is the feedback loop, consisting of two genes $a$ and $b$ that regulate each other's expression. A well-studied example of such a module, in which both regulations are at the transcriptional level, is the λ switch in *Escherichia coli* [17]. Such a transcriptional feedback loop, referred to as the genetic toggle switch, was constructed also using methods of synthetic biology and was shown to exhibit bistability [18]. Subsequent theoretical and numerical studies established the conditions under which bistability takes place in such systems [19–25].

In mixed feedback loops (MFLs), the two genes regulate each other using two different regulation mechanisms. A common form of MFL involves a gene $a$ that expresses a TF and regulates gene $b$ via transcriptional regulation, while gene $b$ transcribes a sRNA molecule and regulates gene $a$ via posttranscriptional regulation by sRNA-mRNA interaction. In general, both the transcriptional regulator and the posttranscriptional regulator can act to either inhibit or activate their target. MFLs in which both regulations are negative (double-negative MFLs) belong to the class of coherent feedback loops in which the number of negative regulations is even. The positive-negative MFLs belong to the class of incoherent feedback loops. In general, coherent feedback loops tend to exhibit bistability while incoherent feedback loops tend to exhibit oscillations, under appropriate parameter settings. A schematic representation of a coherent MFL is shown in Fig. 1.

Integration of the transcriptional regulation network and the network of sRNA-mRNA interactions in *E. coli* has revealed that MFLs play important roles in various cellular contexts [8]. A textbook example of such a module is the coherent MFL that consists of the TF Fur and the sRNA RyhB, involved in iron metabolism [26–28]. Another example of a coherent MFL in *E. coli* consists of the TF Lrp and the sRNA MicF, involved in cellular response to variation in nutrient availability [29].

 

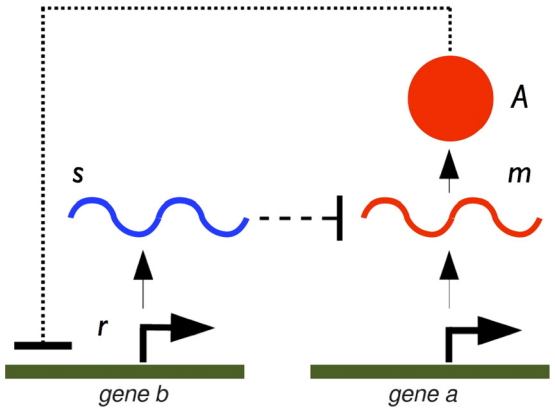


FIG. 1. (Color online) A schematic representation of the mixed feedback loop. Gene $a$ is transcribed into mRNA molecules ($m$), which are translated into transcriptional repressor proteins ($A$). Gene $b$ is transcribed into sRNA molecules ($s$). The $A$ repressors negatively regulate the transcription of gene $b$ by binding to its promoter (the bound repressor is denoted by $r$). The sRNA molecules transcribed from gene $b$ bind to the mRNA molecules of gene $a$ and inhibit their translation. Truncated arrows represent negative regulation.

Other examples of MFLs involving noncoding RNAs (microRNAs) were found in the human regulatory network, playing a role in human granulopoiesis [30], various cancers [31] and monocytic differentiation and maturation [32]. Further examples of MFLs were also found in *Drosophila melanogaster* [33], in *Vibrio harveyi* [34], and in *Caenorhabditis elegans* [35]. The frequent identification of feedback loops and mixed feedback loops in the regulatory networks of various organisms hints at their important regulatory functions [36].

The dynamic behavior of MFLs involving protein-protein interaction was analyzed theoretically using deterministic analysis in the framework of rate equation models [37]. It was shown that within suitable ranges of parameters, the double-negative (coherent) MFL exhibits bistability, while the positive-negative (incoherent) MFL exhibits oscillations. Similar results were recently obtained for MFLs involving sRNAs [38] and microRNAs [39].

Gene regulation processes are affected by fluctuations due to the stochastic nature of biochemical reactions and the fact that some of the molecules involved appear in low copy numbers. Therefore, in order to obtain a more complete understanding of the dynamic behavior of coherent MFLs and the emergence of bistability it is important to analyze these systems using stochastic methods which take into account the discrete nature of the interacting RNAs and proteins as well as the effects of fluctuations. Fluctuations in MFLs were previously characterized using stochastic methods [40,41]. However, the lifetimes of the two bistable states and their dependence on the model parameters have not been studied.

In this paper we present a comprehensive analysis of the dynamics of a mixed coherent MFL involving transcriptional regulation and sRNA-mRNA interaction. The analysis is done using a combination of deterministic and stochastic methods, enabling us to identify the stable states of this system as well as the spontaneous, fluctuation-driven transitions between them. We calculate the average lifetimes of the two bistable states vs parameters such as the components' transcription rates. As expected, we show that as the transcription rate of the mRNA, $g_m$, is increased, the average lifetime of the state dominated by the transcriptional repressor increases, while the average lifetime of the state dominated by the sRNA decreases. Thus, for small values of $g_m$ the system spends most of its time in the sRNA-dominated state, while for large values of $g_m$ it spends most of its time in the state dominated by the transcriptional repressor. This means that in the two limits the domination times of the two regulators are biased towards one of the two bistable states. The biological relevance of these observations is discussed in the context of such MFLs which appear in *E. coli*, the MFL which involves Fur and RyhB, and the MFL which consists of Lrp and MicF. It is shown that the dependence of some relevant rate coefficients on the biological conditions enables the cells to switch to the state which is better suited for the existing conditions and to remain in this state as long as these conditions persist.

The paper is organized as follows. In Sec. II we present a deterministic analysis of the MFL and the results for the range of parameters in which bistability appears. In Sec. III we present a stochastic analysis, calculating the average lifetimes of the two bistable states vs suitable parameters. The biological relevance of the results is discussed in Sec. IV. In Appendix A we present a detailed account of the experimental data we have used and the considerations we have made in order to determine the biologically relevant values of the rate coefficients used in our model. In Appendix B we extend both the deterministic and stochastic stability analyses to a broader family of parameter variations and to the case in which the transcriptional repressor exhibits cooperative binding.

## II. DETERMINISTIC ANALYSIS

Consider an MFL in which gene $a$ encodes a transcription factor and gene $b$ encodes a small RNA molecule. Gene $a$ negatively regulates gene $b$ by transcriptional regulation, while gene $b$ negatively regulates gene $a$ posttranscriptionally via sRNA-mRNA interaction. In this system gene $a$ is transcribed into mRNA molecules, which are translated into transcriptional repressor proteins. Gene $b$ is transcribed into sRNA molecules. The transcriptional repressors $A$ negatively regulate gene $b$ by binding to its promoter site, while the sRNA molecules negatively regulate gene $a$ by binding to its mRNA molecules, destabilizing them and inhibiting their translation.

Here we describe the dynamics of an MFL with one TF gene and one sRNA gene, using rate equations. We denote the levels or copy numbers of the sRNA and mRNA molecules in the cell by $s$ and $m$, respectively. The level of the sRNA-mRNA complex is denoted by $C$. The number of free $A$ proteins is denoted by $A$. The number of $A$ proteins that are bound to the promoter site of gene $b$ is denoted by $r$. For simplicity, we first consider the case in which the regulation is performed by a single copy of the bound repressor. In this case, $r$ takes values in the range $0 \leqslant r \leqslant 1$.

The rate coefficients $g_m$ and $g_s$ denote the transcription rates of genes $a$ and $b$, respectively. The translation rate of gene $a$, namely, the generation rate of $A$ proteins per copy of

TABLE I. The processes and respective rates in the MFL module.

| | Process | Rate |
|---|---|---|
| 1 | $\emptyset \rightarrow m$ | $g_m$ |
| 2 | $\emptyset \rightarrow s$ | $g_s(1-r)$ |
| 3 | $m \rightarrow m + A$ | $g_A m$ |
| 4 | $m + s \rightarrow C$ | $c_{ms} ms$ |
| 5 | $A \rightarrow r$ | $c_g A(1-r)$ |
| 6 | $r \rightarrow A$ | $u_g r$ |
| 7 | $m \rightarrow \emptyset$ | $d_m m$ |
| 8 | $A \rightarrow \emptyset$ | $d_A A$ |
| 9 | $s \rightarrow \emptyset$ | $d_s s$ |
| 10 | $C \rightarrow m + s$ | $u_c C$ |
| 11 | $C \rightarrow \emptyset$ | $d_c C$ |

the mRNA molecule is denoted by $g_A$. The degradation rates of the sRNAs, mRNAs, and the $A$ proteins are denoted by $d_s$, $d_m$, and $d_A$, respectively. The binding rate of $A$ proteins to the promoter site of gene $b$ is denoted by $c_g$ and their dissociation rate from the promoter is denoted by $u_g$. The binding rate of sRNA and mRNA molecules to form a complex is denoted by $c_{ms}$. The sRNA-mRNA complex degrades at rate $d_c$, or dissociates into its sRNA and mRNA components at rate $u_c$. The processes taking place in the MFL and their rates are listed in Table I.

In Appendix A we consider the biologically relevant range of values of each of the rate coefficients used in the analysis of the MFL. These values are determined on the basis of experimental results and related considerations and interpretations. For the calculations and simulations presented below we chose a default value for each parameter, within the biologically relevant range. These default parameter values, $g_m = 0.007$, $g_s = 0.43$, $g_A = 0.05$, $d_m = 0.003$, $d_s = 0.0008$, $d_A = 0.001$, $c_{ms} = 0.02$, $c_g = 0.08$, and $u_g = 0.01$, are used in all the figures presented in this paper (unless stated otherwise). All the parameters are in units of $s^{-1}$.

The rate equations that describe this system take the form

$$\frac{dm}{dt} = g_m - d_m m - c_{ms} ms + u_c C \tag{1a}$$

$$\frac{ds}{dt} = g_s(1-r) - d_s s - c_{ms} ms + u_c C \tag{1b}$$

$$\frac{dA}{dt} = g_A m - d_A A - c_g A(1-r) + u_g r \tag{1c}$$

$$\frac{dr}{dt} = c_g A(1-r) - u_g r \tag{1d}$$

$$\frac{dC}{dt} = c_{ms} ms - d_c C - u_c C, \tag{1e}$$

where Eqs. (1a) and (1b) account for the time-dependent levels of the mRNA and sRNA molecules, respectively. Each of these equations includes a transcription term and a degradation term. They also include binding terms, which describe the formation rate of the sRNA-mRNA complex, and a term which represents the dissociation of the complex. The transcription term of $s$ includes the factor $1-r$, which accounts for the fact that transcription takes place only when there is no $A$ repressor bound to the $b$ promoter. Equation (1c) accounts for the time-dependent level of the free $A$ protein, and includes translation and degradation terms as well as terms describing the binding (unbinding) to (from) the $b$ promoter. Equation (1d) accounts for the level of $A$ proteins which are bound to the $b$ promoter. Equation (1e) accounts for the level of the sRNA-mRNA complex.

The rate equations can be solved by direct numerical integration. For fixed values of the parameters and for a given choice of the initial conditions, the system tends to converge to a steady state. Coherent feedback loops such as the MFL tend to exhibit bistability within a suitable range of parameters. In such cases, the steady state to which the rate equations converge depends on the initial conditions. Within the rate equation model, once the system converges to one of the bistable states, it remains there and does not switch to the other state.

Under steady state conditions (or in the limit in which the formation and dissociation processes of the sRNA-mRNA complex are fast) the effect of the dissociation process on the RNA and protein levels can be accounted for by a suitable adjustment of the binding rate coefficient $c_{ms}$. Therefore, the dissociation process is expected to be of secondary importance and does not affect the essential properties of the MFL.

In the analysis presented below it is assumed, for simplicity, that the dissociation rate $u_c = 0$, namely, once an sRNA-mRNA complex is formed, it goes to degradation rather than dissociating into its sRNA and mRNA components. Under this assumption, the level of the sRNA-mRNA complex, $C$, has no effect on the levels of other components in the MFL. The assumption $u_c = 0$, and the subsequent irrelevance of $d_c$, will hold for the rest of the paper, unless stated otherwise, such as in Appendix B. Therefore, the set of four equations (1a)–(1d) can be integrated numerically or solved separately from Eq. (1e).

Under steady state conditions, the time derivatives on the left hand side of Eqs. (1) vanish, and the rate equations are reduced to a set of coupled algebraic equations. These equations can be transformed into a single cubic equation of the form

$$\left(m - \frac{g_m}{d_m}\right)\left(m + \frac{d_s}{c_{ms}}\right)\left(m + \frac{u_g}{c_g}\frac{d_A}{g_A}\right) + \frac{u_g}{c_g}\frac{d_A}{g_A}\frac{g_s}{d_m} m = 0. \tag{2}$$

For convenience we define the following dimensionless parameters: $M = g_m/d_m$, $D = d_s/c_{ms}$, $K = u_g d_A/(c_g g_A)$, and $S = g_s/d_m$. The parameter $M$ represents the average number of mRNA molecules in the cell in the case that they are not regulated by sRNAs. The parameter $D$ is the ratio between the probabilites that a single sRNA molecule will degrade or bind to a single mRNA target. Therefore, $D$ tends to decrease as the strength of the regulation by sRNA molecules increases. The parameter $K$ is inversely proportional to the level of $A$ proteins (when unregulated) and to their binding affinity to the $b$ promoter. Therefore, $K$ decreases as the transcriptional regulation of gene $b$ becomes stronger. The parameter $S$ represents the number of sRNA molecules which are transcribed during the average lifetime of an mRNA molecule. Using these parameters, we obtain a cubic equation

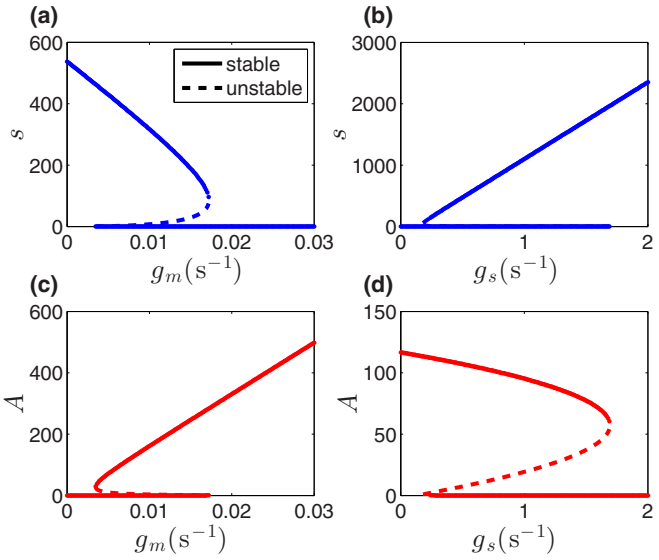


FIG. 2. (Color online) Bifurcation diagrams showing the levels of $s$ and $A$ as functions of the parameters $g_m$ (a),(c) and $g_s$ (b),(d). Solid lines represent stable solutions and dashed lines represent unstable solutions.

for $m$ of the form

$$m^3 + a_2 m^2 + a_1 m + a_0 = 0, \tag{3}$$

where $a_0 = -KDM$, $a_1 = K(D+S-M) - MD$, and $a_2 = D + K - M$. Depending on the values of the parameters, the system may exhibit either a single steady state or bistability.

To analyze the existence and stability of the steady states of the MFL, it is useful to consider the bifurcation diagrams, presenting the steady state levels of $A$ and $s$ as a function of different parameters of the model. The stability of the solutions can be determined from the Jacobian of the set of rate equations and its eigenvalues.

In Figs. 2(a) and 2(c) we present the levels of the sRNA and the $A$ protein under steady state conditions as a function of $g_m$, obtained analytically from the rate equations. For small values of $g_m$, a single steady state is observed, which is dominated by the sRNA. As $g_m$ increases, a bifurcation takes place and a second steady state, dominated by $A$ proteins, appears. A second bifurcation occurs at larger $g_m$ value, beyond which only a single stable steady state remains, which is dominated by the $A$ proteins. Similar results are presented in Figs. 2(b) and 2(d) as a function of $g_s$.

In order to extend and exemplify the robustness of the results presented above, in Appendix B we present the bifurcation diagrams of the MFL obtained for different binding and unbinding kinetics of the TF to the sRNA promoter, different values of dissociation kinetics of the sRNA-mRNA complex, and different values of cooperativity of the TF to the sRNA promoter. In all cases, we observe a range of parameters in which bistability takes place.

## III. STOCHASTIC ANALYSIS

In order to account for the effects of fluctuations in the MFL we analyze its dynamics using the master equation. Here the levels of the RNA molecules and protein take integer values, namely, $m,A,s \in \mathbb{N}_0$, while the level of the bound repressor $r \in \{0,1\}$. The master equation accounts for the temporal variation of the probability distribution $P(m,A,r,s)$. It takes the form

$$\begin{aligned}
&\frac{dP(m,A,r,s)}{dt} \\
&= g_m[P(m-1,A,r,s) - P(m,A,r,s)] \\
&\quad + g_s\delta_{r,0}[P(m,A,r,s-1) - P(m,A,r,s)] \\
&\quad + g_A m[P(m,A-1,r,s) - P(m,A,r,s)] \\
&\quad + c_{ms}[(m+1)(s+1)P(m+1,A,r,s+1) - ms\,P(m,A,r,s)] \\
&\quad + c_g[(A+1)\delta_{r,1}P(m,A+1,0,s) - A\delta_{r,0}P(m,A,0,s)] \\
&\quad + u_g[\delta_{r,0}P(m,A-1,1,s) - \delta_{r,1}P(m,A,1,s)] \\
&\quad + d_m[(m+1)P(m+1,A,r,s) - m\,P(m,A,r,s)] \\
&\quad + d_A[(A+1)P(m,A+1,r,s) - A\,P(m,A,r,s)] \\
&\quad + d_s[(s+1)P(m,A,r,s+1) - s\,P(m,A,r,s)],
\end{aligned} \tag{4}$$

where $\delta_{i,j} = 1$ for $i = j$ and 0 otherwise.

The first (second) term in this equation describes the transcription of mRNA (sRNA) molecules. The third term accounts for the translation of mRNA molecules into $A$ proteins. The term involving $c_{ms}$ describes the binding of sRNA and mRNA molecules, to form an sRNA-mRNA complex. The terms involving $c_g$ and $u_g$ describe the binding or dissociation of $A$ proteins to or from the promoter site of gene $b$, respectively. The last three terms correspond to the degradation of mRNA molecules, $A$ proteins, and sRNA molecules, respectively.

In order to examine the properties of the steady state solution of the master equation, it is useful to consider the marginal probability distribution

$$P(A,s) = \sum_m \sum_r P(m,A,r,s). \tag{5}$$

In the formulation based on the master equation, the criterion for bistability is that the steady state solution $P(A,s)$ exhibits two distinct peaks, separated by a gap in which the probabilities are low. The locations of these peaks on the $(A,s)$ plane correspond to the two bistable solutions of the rate equations.

In order to obtain the switching times between the two bistable states and estimate the probability distributions of the different possible discrete states of the system, we perform Monte Carlo (MC) simulations using the Gillespie algorithm [42]. This is a kinetic MC approach, namely, an algorithm that generates "paths" of the stochastic process. At each time step the next move is drawn from all possible processes that may take place at that point, where each step is endowed with a suitable weight. After each move, the elapsed time is properly advanced, the list of available processes is updated, and their new rates are evaluated.

In Fig. 3 we present the probability distribution $P(A,s)$, generated by performing MC simulations ($10^7$ s each), and quantifying the relative fraction of time in which the system is found in each discrete $P(A,s)$ state, averaged over initiations of the system at both the sRNA- and TF-dominated states. The probability distribution is presented for conditions under which

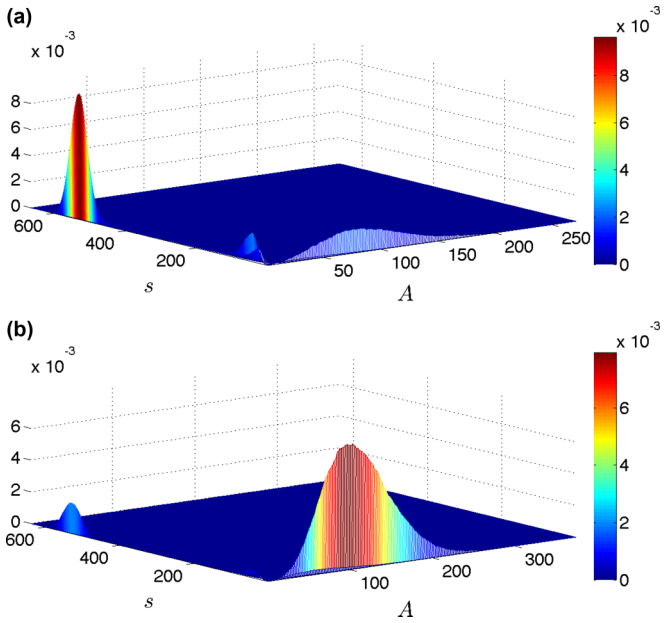


FIG. 3. (Color online) The MFL probability distribution $P(A,s)$ (a) for the state dominated by the sRNA regulator (obtained for $g_m = 0.0058\ \mathrm{s}^{-1}$) and (b) for the state dominated by the transcriptional repressor (obtained for $g_m = 0.0071\ \mathrm{s}^{-1}$).

the system is dominated by the sRNA regulator [Fig. 3(a)] and for conditions under which it is dominated by the transcriptional repressor [Fig. 3(b)]. In both cases the distribution exhibits two peaks representing the two bistable states. In the former case the peak dominated by sRNA molecules is large and the peak dominated by transcriptional repressors is small, while in the latter case the situation is reversed. The volume of each peak represents the cumulative probability of microscopic states associated with the corresponding state of the system. It also represents the fraction of the time in which the system is expected to reside in that state over multiple realizations.

We denote the mean lifetimes of the bistable states dominated by the sRNA and by the transcriptional repressor by $\tau_s$ and $\tau_A$, respectively. To obtain the values of $\tau_s$ ($\tau_A$) we initialize the system in the state dominated by the sRNA (transcriptional repressor) and evaluate the average time elapsed until a transition to the $A$- ($s$-) dominated state has occurred. The transition between states is defined as the point in which the level of the previous minority species exceeds that of the dominant species.

In Fig. 4 we present a typical result of an MC simulation of the MFL. The system is clearly bistable, with spontanous fluctuation-driven switching transitions. In the sRNA-dominated state there are failed switching attempts, corresponding to the third, unstable steady state, in which the sRNA level is reduced, but is then recovered. In the $A$-dominated state, both the mRNA and protein levels exhibit large fluctuations, accompanied by fast binding (unbinding) of $A$ proteins to (from) the $b$ promoter.

To examine the dependence of the lifetimes of the two bistable states on parameters, we present in Fig. 5 the lifetime of the sRNA-dominated state, $\tau_s$, as a function of the transcription rates of the mRNA and sRNA. As the

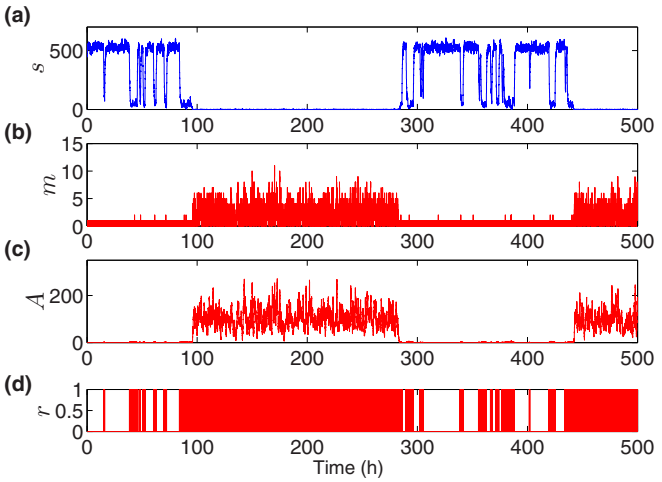


FIG. 4. (Color online) The levels of the sRNA molecules (a), mRNA molecules (b), free $A$ repressors (c), and bound repressors (d) vs time in the MFL, obtained from Monte Carlo simulations. Failed attempts to transition from the $s$- to the $A$-dominated state are observed, following periods in which the $s$ promoter is occupied by the transcriptional repressor.

transcription rate $g_m$ is increased, the switching rate from the state dominated by the sRNA to the state dominated by the transcriptional repressor increases and the lifetime $\tau_s$ of the sRNA-dominated state decreases [Fig. 5(a)]. On the other hand, when the transcription rate of the sRNA, $g_s$,

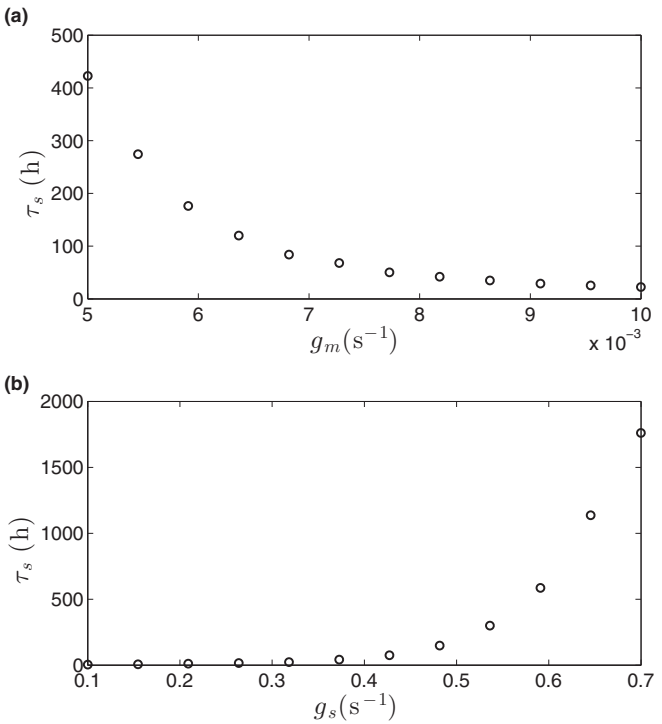


FIG. 5. The average lifetime of the sRNA-dominated state, $\tau_s$, as a function of the parameters $g_m$ (a) and $g_s$ (b), obtained from MC simulations. The lifetime $\tau_s$ monotonically decreases with $g_m$ and monotonically increases with $g_s$. Each data point was averaged over 1000 MC runs.

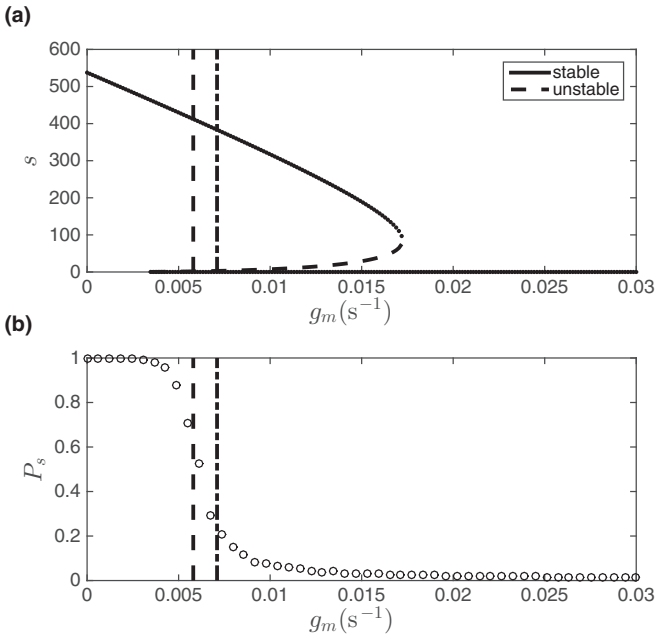


FIG. 6. (a) The sRNA level $s$ as a function of the transcription rate $g_m$, obtained from the rate equations. (b) The fraction of time $P_s$ that the system resides in the sRNA-dominated state vs $g_m$, obtained from MC simulations. The dependence of $P_s$ on $g_m$ is of the form of a decreasing sigmoid function. Two vertical lines mark the $g_m$ values, as shown in Fig. 3, for the state dominated by the sRNA regulator for which $P_s > 0.5$ (obtained for $g_m = 0.0058\ \mathrm{s}^{-1}$, marked by a dashed line), and for the state dominated by the transcriptional repressor for which $P_s < 0.5$ (obtained for $g_m = 0.0071\ \mathrm{s}^{-1}$, marked by a dash-dotted line).

is increased, the lifetime of the sRNA-dominated state, $\tau_s$, increases [Fig. 5(b)].

Further insight into the balance between the two bistable states can be obtained by evaluating the fraction of the time in which the system resides in each state. The fraction of time in which the sRNA is dominant is given by

$$P_s = \frac{\tau_s}{\tau_A + \tau_s}, \tag{6}$$

while the fraction of time in which the transcriptional repressor is dominant is $P_A = 1 - P_s$.

In Fig. 6(a) we present the bifurcation diagram for the sRNA level vs $g_m$, obtained from the rate equations, showing the range of $g_m$ values in which bistability takes place. In Fig. 6(b) we present the fraction of time $P_s$ in which the system resides in the sRNA-dominated state vs $g_m$, obtained from MC simulations. $P_s$ follows a decreasing sigmoid function vs $g_m$. In the limit in which $g_m$ is small the system spends most of its time in the sRNA-dominated state, while in the large $g_m$ limit it spends most of its time in the state dominated by the transcriptional repressor. It is found that in both limits, the MFL is biased towards one of the steady states.

In Appendix B, we present results for $P_s$ when the binding and unbinding kinetics of the TF to the sRNA promoter are varied, for different values of dissociation kinetics of the sRNA-mRNA complex, and for different values of cooperativity of the TF to the sRNA promoter. In all cases, $P_s$ follows a sigmoid function, either decreasing or increasing, in accordance with the bifurcation diagrams for each parameter setting, as discussed in Appendix B.

## IV. DISCUSSION

Bistability plays an important role in many biological systems. At the population level, it gives rise to phenotypic diversity, namely, the coexistence of two phenotypes in populations of genetically identical cells [43,44]. This may enhance the survivability of the cell population since different phenotypes may be advantageous under different conditions. The fluctuation-driven transitions between the two bistable states are crucial because they enable mixing between the two subpopulations and provide a mechanism for the adjustment of their relative sizes according to the external conditions. The relative sizes of the two subpopulations are determined by the lifetimes of the two bistable states as well as by other factors such as the cell division rates. For example, it was found that only 10%–20% of cells in a culture of *Bacillus subtilis* are in the competent state, namely, express the proteins needed for the uptake of DNA, while all other cells are in the noncompetent state [45,46]. The gene regulation module which regulates this bistable behavior was studied experimentally and the fluctuation-driven transitions were analyzed using stochastic simulations [44,47].

We have performed deterministic and stochastic analyses of a genetic regulatory module which gives rise to bistability: the double-negative mixed feedback loop involving transcriptional regulation and posttranscriptional regulation via sRNA-mRNA interaction. Using deterministic methods we identified the range of parameters in which this system exhibits bistability. Using stochastic simulations we calculated the mean lifetimes $\tau_s$ and $\tau_A$ of the bistable states dominated by the sRNA and the TF, respectively. From these results we obtained the fractions of the time which the cell spends in the sRNA-dominated state ($P_s$) and in the TF-dominated state ($P_A$). We have shown that $P_s$ follows a sigmoid function vs parameters such as transcription rates and binding and unbinding rates. The sigmoid functions exhibit a limit in which $P_s \to 1$, where the cell spends most of the time in the sRNA-dominated state and an opposite limit in which $P_s \to 0$, where the cell spends most of the time in the TF-dominated state. Different values of $P_s$ may be beneficial for the cell under different biological conditions, yielding, at the population level, a bimodal distribution with different relative sizes of the subpopulations.

Our results show that, by changing the values of the rate coefficients, the cell can switch from conditions in which the sRNA-dominated state exhibits a long relative lifetime to conditions in which the TF-dominated state exhibits a long relative lifetime. Below we present two examples of MFLs in bacteria, in which relevant rate coefficients are directly adjusted by external conditions. More specifically, in these MFLs the affinity of the TF for the sRNA promoter depends on the availability of certain molecules. Under conditions in which the TF exhibits high affinity, the TF-dominated state will exhibit a long relative lifetime and most of the cells will switch to this state. Under the opposite conditions, in which the affinity of the TF for the sRNA promoter is low, the

sRNA-dominated state will exhibit a long relative lifetime and most of the cells will reside in this state. Such a mechanism thus enables the majority of cells to adjust to the state which is better suited for the existing conditions and remain in this state in a stable fashion as long as these conditions persist. Once the external conditions change and the other state becomes preferable, this mechanism enables the cells to quickly switch to the other state and remain in that state as long as the new conditions persist. The mechanism described above can be exemplified by the following two examples.

An important example of a double-negative MFL which appears in *E. coli*, consists of the genes *fur*, encoding a transcriptional repressor, and *ryhB*, encoding an sRNA molecule. In this module, Fur negatively regulates the transcription of *ryhB* by binding to its promoter, while *ryhB* negatively regulates the expression of *fur* by posttranscriptional regulation. In the presence of iron, the Fur repressor is active, binding to the promoter regions of its targets with ferrous iron ($Fe^{2+}$) as a cofactor, repressing the transcription of the RyhB sRNA, as well as other genes involved in iron metabolism [26–28]. When iron supply is limited, Fur becomes inactive and RyhB is transcribed. Fur synthesis is translationally coupled to that of an upstream open reading frame, whose translation is downregulated by RyhB [28]. When the iron level increases and the stress condition is removed, the level of Fur is restored and overrides the RyhB sRNA [27].

Another important example of a double-negative MFL in *E. coli* consists of the global transcriptional regulator Lrp and the sRNA MicF [29]. Lrp is a global regulator which activates genes that need to be expressed under nutrient-poor conditions while repressing genes that need to be expressed under nutrient-rich conditions [48,49]. In this module, Lrp negatively regulates the transcription of *micF* by binding to its promoter, while *micF* negatively regulates the expression of *lrp* by posttranscriptional regulation. The regulatory activity of Lrp is modulated by the cellular leucine level, which is typically high under nutrient-rich conditions and low under nutrient-poor conditions. Leucine binding tends to reduce the efficiency of Lrp as a transcriptional repressor, which means that Lrp is an efficient repressor under nutrient-poor conditions and an inefficient repressor under nutrient-rich conditions. Accordingly, it was shown that Lrp is highly expressed under nutrient-poor conditions, while MicF is highly expressed under nutrient-rich conditions.

## ACKNOWLEDGMENTS

This work was supported by grants from the Israel Science Foundation and the Israel Ministry of Science and Technology to H.M. M.N. is grateful to the Azrieli Foundation for the award of an Azrieli Fellowship.

## APPENDIX A: RATE COEFFICIENTS

The equations that describe the MFL include a large number of rate coefficients for the rates of the transcription, translation, binding, unbinding, and degradation processes. To obtain results and predictions that are biologically meaningful, one should use rate coefficients that are in the biologically relevant range. While the analysis performed in this paper is quantitative, the conclusions are of a qualitative nature and describe the generic behavior of the MFL. Below we discuss in more detail the considerations we have made in order to identify the biologically relevant range of each parameter.

### 1. Transcription and degradation rates of mRNA molecules

Previous analyses have revealed that the rate limiting step in the transcription is usually the delay between the binding of RNA polymerase to the promoter site and the beginning of the elongation process [50]. Measurements have shown that this time lag exhibits great variation between different genes and under different conditions and takes values between 20 s and 10 min. The delay time can be represented by the transcription initiation rate, taking values in the range $0.001 \leqslant g_m \leqslant 0.05$ molecules per second. Recent measurements of mRNA molecules in single cells showed that for the gene that was studied, an mRNA molecule is produced every 7 min, which amounts to a transcription rate of $g_m = 0.0024$ ($s^{-1}$) [51]. The half-life of mRNA is typically in the range between 30 and 300 (s). This yields mRNA degradation rates in the range $0.003 \leqslant d_m \leqslant 0.03$ ($s^{-1}$).

### 2. Transcription and degradation rates of sRNA molecules

An example of a small RNA in *E. coli*, on which extensive experimental measurements have been performed, is OxyS. This sRNA appears in high copy numbers [52]. In the absence of target mRNAs, it was found to have a half-life of 12–15 min, which is longer than most mRNAs. In order to allow for variations between different sRNAs, we chose a broader range of half-life values, translating to sRNA degradation rates in the range $0.0002 \leqslant d_s \leqslant 0.002(s^{-1})$.

Values reported for generation rates of various sRNAs were in the range $0.02 \leqslant g_s \leqslant 7.5$ ($s^{-1}$). The lower limit was reported in [4]. The upper limit was obtained by assuming that the steady state level of oxyS was due to synthesis and degradation processes, $g_s = s \times d_s = 4500 \times (0.0005 - 0.00167\ s^{-1})$ [52] $= 2.5$–$7.5\ s^{-1}$ [53].

### 3. Protein synthesis and degradation rates

Measurements of protein synthesis rates are reported in Ref. [54]. It was shown that a protein can be translated from each mRNA molecule every 3–4 s. To cover a broad range of biologically relevant translation rates, we take the range of 2–20 s. This corresponds to translation rate coefficients in the range $0.05 \leqslant g_A \leqslant 0.5$ ($s^{-1}$).

Transcription factors are usually short lived, with half-lives of a few minutes. Thus, we consider degradation rates in the range $0.001 \leqslant d_A \leqslant 0.05$ ($s^{-1}$).

### 4. Binding rates of sRNA molecules to their mRNA targets

Measurements of the binding of the sRNA OxyS to its mRNA target *fhlA*, performed *in vitro*, are reported in Ref. [52]. In these experiments 2 nM of the OxyS sRNA were mixed with different concentrations of the *fhlA* mRNA. After 5 min the concentration of free OxyS was measured. It was found that when the concentration of the *fhlA* mRNA was 25 nM, half of the OxyS molecules were bound after 5 min. This was done

*in vitro*, where the synthesis of new sRNA and mRNA molecules as well as their degradation were suppressed. Denoting the level of OxyS by $s$ and of the *fhla* mRNA by $m$, the dynamics can be described by

$$\frac{ds}{dt} = -c_{ms} m s, \qquad \frac{dm}{dt} = -c_{ms} m s. \tag{A1}$$

This means that under these conditions the difference between the levels of $m$ and $s$ remains constant. Assuming that the initial levels at time $t = 0$ satisfy $m_0 > s_0$, we can solve this equation and obtain

$$s(t) = \frac{(m_0 - s_0)s_0}{m_0 \exp[c_{ms}(m_0 - s_0)t] - s_0}, \qquad m(t) = \frac{(m_0 - s_0)m_0}{m_0 - s_0 \exp[-c_{ms}(m_0 - s_0)t]}. \tag{A2}$$

Setting the initial conditions and fitting the binding rate coefficient $c_{ms}$ such that after 5 min the sRNA concentration $s$ goes down to one-half of the initial concentration $s_0$, we obtain that $c_{ms} = 9.45 \times 10^{-5}$ (nM s)$^{-1}$. Taking the *E. coli* cell volume as $10^{-15}$ l, we obtain 1 nM = 0.6 molecules per cell, giving $c_{ms} = 0.0002(\mathrm{s}^{-1})$. Since this experiment was carried out without Hfq, which is a catalyst of the reaction, it is reasonable to take a range of $c_{ms}$ values which express faster binding. This would most likely also account for variations in the binding rates of other sRNA molecules to other mRNAs. We therefore take the range $0.001 \leqslant c_{ms} \leqslant 0.02$ (s$^{-1}$).

#### 5. Transcription factor binding and unbinding rates

The binding and unbinding rates of two transcription factors in two *E. coli* strains to (from) their specific promoter sites on the DNA were measured in Ref. [55]. Using surface plasmon resonance, which can monitor the time-dependent changes in concentrations, they found binding rates of 0.09–0.14 (s$^{-1}$). This means that a transcription factor would bind to the DNA within 7–11 s. Measuring the ratio between bound and free DNA yields the ratio between the binding and dissociation rates. The values that were obtained for the dissociation rate are in the range of 0.001–0.002 (s$^{-1}$). This in turn means that a transcription factor stays bound to the promoter site for 1000 to 2000 s. To make the range more dynamic and account for weaker transcriptional repression we choose the ranges $0.05 \leqslant c_g \leqslant 0.25$ (s$^{-1}$), and $0.001 \leqslant u_g \leqslant 0.01$(s$^{-1}$).

## APPENDIX B: EXTENDED STABILITY ANALYSIS

Here we investigate how the MFL bifurcation diagram (a result of the deterministic analysis) and the fraction of time $P_s$ in which the system resides in the sRNA-dominated state (a result of the stochastic analysis) are affected by a broad family of parameter variations and modifications of the dynamic processes. In Fig. 2 we showed the bifurcation diagrams for the parameters $g_m$ and $g_s$, representing the transcription rates of the TF and sRNA, respectively. In Fig. 6 we showed $P_s$ as a function of the parameter $g_m$. Here we further present the bifurcation diagrams and the plots of $P_s$ for the binding and unbinding rates of the TF to the sRNA promoter, denoted by $c_g$ and $u_g$, respectively, and the transcription rate of the sRNA, denoted by $g_s$. In addition, we examine the effect of both the dissociation rate of the sRNA-mRNA complex, denoted by $u_c$, and the cooperativity of the binding of the TF to the sRNA promoter, which is characterized by the Hill coefficient $\alpha$. The rate equations describing the MFL with cooperative binding take the form

$$\frac{dm}{dt} = g_m - d_m m - c_{ms} m s + u_c C, \tag{B1a}$$

$$\frac{ds}{dt} = g_s(1 - r) - d_s s - c_{ms} m s + u_c C, \tag{B1b}$$

$$\frac{dA}{dt} = g_A m - d_A A - \alpha c_g A^{\alpha}(1 - r) + \alpha u_g r, \tag{B1c}$$

$$\frac{dr}{dt} = c_g A^{\alpha}(1 - r) - u_g r, \tag{B1d}$$

$$\frac{dC}{dt} = c_{ms} m s - d_c C - u_c C. \tag{B1e}$$

For the results presented below, we take the following default parameter values: $g_m = 0.007$, $g_s = 0.43$, $g_A = 0.05, d_m = 0.003, d_s = 0.0008, d_A = 0.001, c_{ms} = 0.02, c_g = 0.08$, $u_g = 0.01$, $d_c = 0.003$, $u_c = 0$, and $\alpha = 1$. All the parameters are in units of s$^{-1}$, except for $\alpha$, which is dimensionless.

In Figs. 7(a)–7(c) and 7(d)–7(f) we present the levels of the sRNA and the $A$ protein under steady state conditions as functions of $c_g$, $u_g$, and $g_s$, respectively, obtained analytically from the rate equations. The ranges of $c_g$, $u_g$, and $g_s$ either agree with or are within those reported in Appendix A. As expected, the effect of $c_g$ (binding of the TF to the sRNA promoter) opposes that of $u_g$ (unbinding); as $c_g$ increases or $u_g$ decreases, the TF strengthens its repressive role over the sRNA. For example, for small values of $u_g$, a single steady state, dominated by the TF, is observed. As $u_g$ increases, a bifurcation takes place and a second steady state, dominated by the sRNA, appears. As $g_s$ increases, the sRNA strengthens relative to the TF, expressed by the bifurcation diagram in Figs. 7(c) and 7(f) [which was also presented and discussed in the main text (Fig. 2)]. In Figs. 7(g)–7(i) we present $P_s$ as a function of $c_g$, $u_g$, and $g_s$, respectively. In all cases, $P_s$ exhibits the sigmoid shape shown in Fig. 6 for variation in the parameter $g_m$. As expected, and consistent with the bifurcation analysis, the probability of the MFL occupying the $s$-dominated state decreases with $c_g$ and increases with $u_g$ and $g_s$.

Next, we consider the effect of the dissociation rate of the sRNA-mRNA complex, denoted by $u_c$, on the stability of the MFL. In Figs. 8(a)–8(c) and 8(d)–8(f) we present the bifurcation diagram showing the levels of $s$ and $A$ as a function of $g_m$, for different values of $u_c$ ($u_c = 0, 0.01, 0.02$). The range of $g_m$ is within that presented in Appendix A. As $g_m$ decreases, a single TF-dominated state bifurcates, and a second sRNA-dominated state appears. This bifurcation occurs for lower values of $g_m$ as $u_c$ increases [Figs. 8(a)–8(f)]. The curve of $P_s$ exhibits a sigmoid shape that decreases with $g_m$ [Figs. 8(g)–8(i)]. Consistent with the deterministic analysis, the probability of the MFL residing in the $s$-dominated state for higher $u_c$ values decreases for lower values of $g_m$.

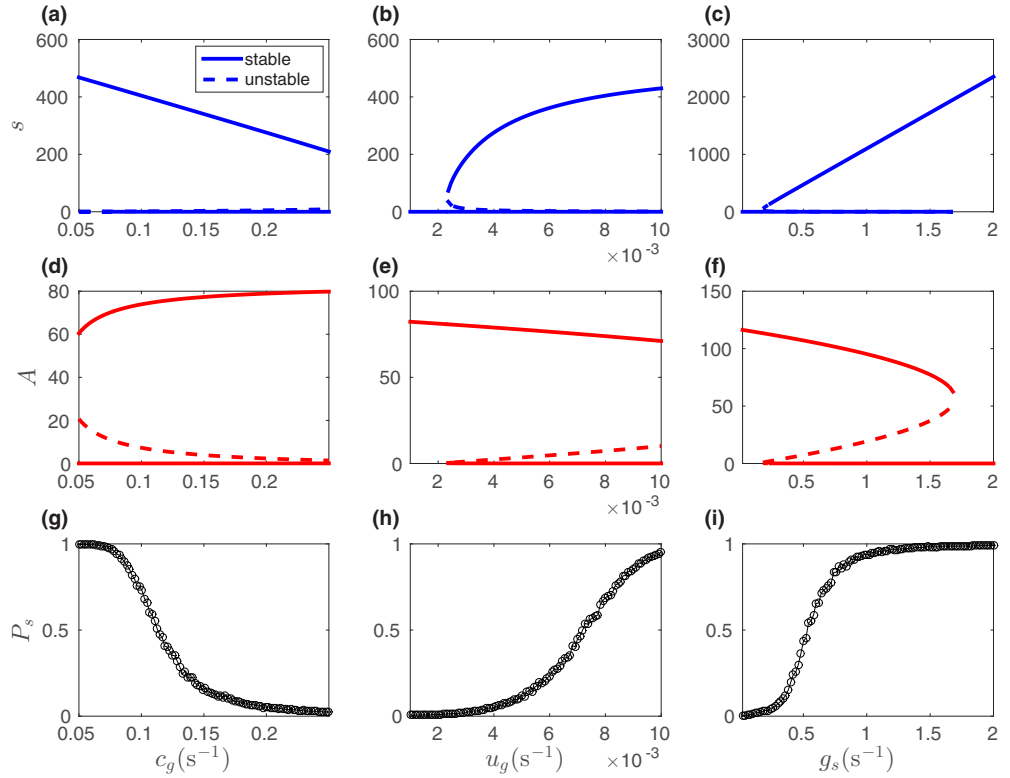


FIG. 7. (Color online) Stability analysis for different $c_g$, $u_g$, and $g_s$ values. (a)–(f) Bifurcation diagrams showing the levels of $s$ and $A$ as a function of the parameters $c_g$ (a),(d), $u_g$ (b),(e), and $g_s$ (c),(f). (g)–(i) $P_s$ curves as a function of $c_g$ (g), $u_g$ (h), and $g_s$ (i). Solid lines represent stable solutions and dashed lines represent unstable solutions.

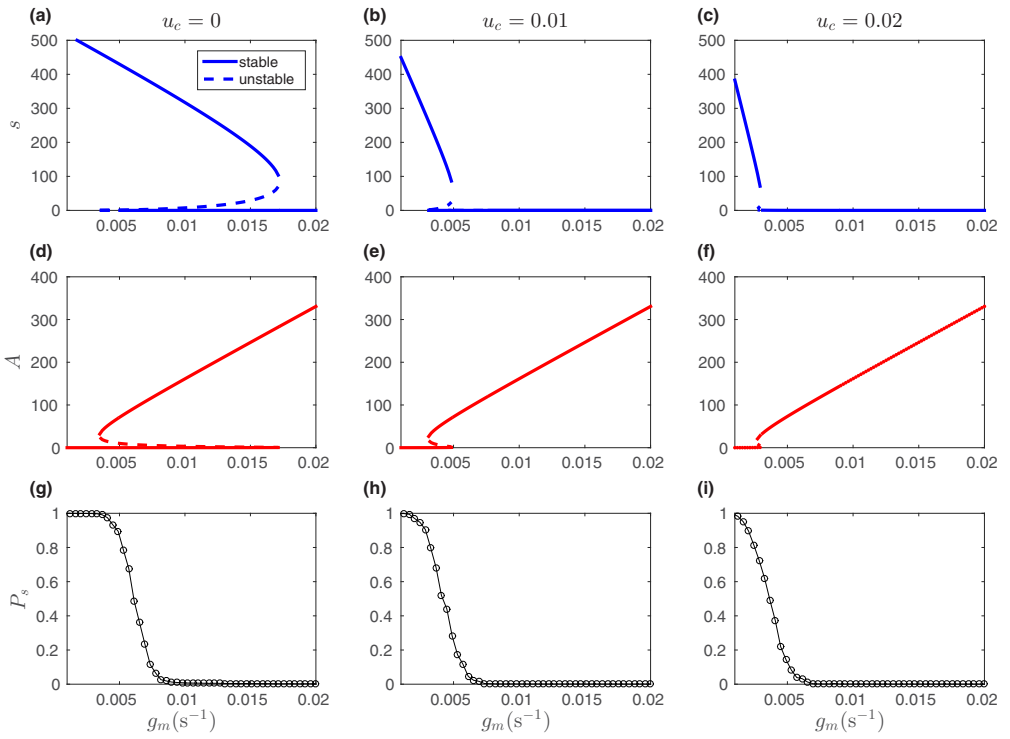


FIG. 8. (Color online) Stability analysis for different $u_c$ values. (a)–(f) Bifurcation diagrams showing the levels of $s$ and $A$ as a function of the parameter $g_m$, for different values of $u_c$. (g)–(i) $P_s$ curves as a function of $g_m$ for different values of $u_c$. The results are presented for different values of $u_c$: $u_c = 0$ (a),(d),(g), $u_c = 0.01$ (b),(e),(h), and $u_c = 0.02$ (c),(f),(i). Solid lines represent stable solutions and dashed lines represent unstable solutions.

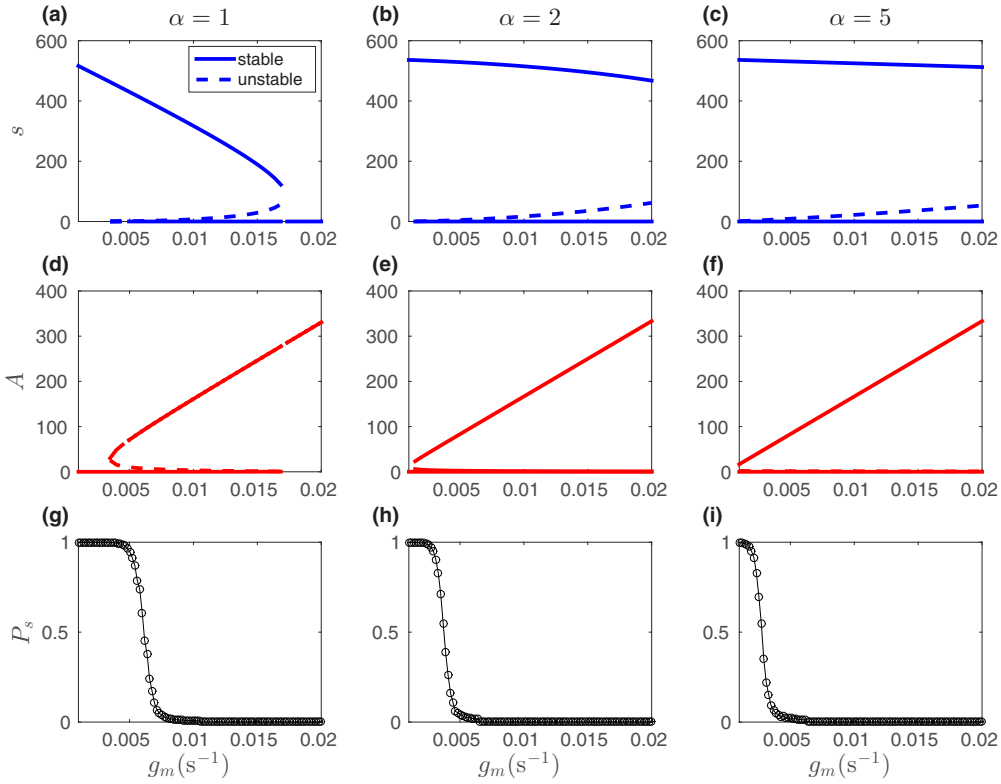


FIG. 9. (Color online) Stability analysis for different $\alpha$ values. (a)–(f) Bifurcation diagrams showing the levels of $s$ and $A$ as a function of the parameter $g_m$, for different values of $\alpha$. (g)–(i) $P_s$ curves as a function of $g_m$ for different values of $\alpha$. The results are presented for different values of $\alpha$: $\alpha = 1$ (a),(d),(g), $\alpha = 2$ (b),(e),(h), and $\alpha = 5$ (c),(f),(i). Solid lines represent stable solutions and dashed lines represent unstable solutions.

Finally, we consider the effect of the cooperativity, as expressed by the Hill coefficient $\alpha$ in Eq. (B1), of the binding of the TF protein to the sRNA promoter on the stability. In Figs. 9(a)–9(c) and 9(d)–9(f) we present the bifurcation diagram showing the levels of $s$ and $A$ as a function of $g_m$, for different values of $\alpha$ ($\alpha = 1,2,5$). For larger values of $\alpha$, $A$ exhibits a nonzero steady state for lower $g_m$ values, leading to the decrease in the value of $g_m$ for which the sigmoid-shaped $P_s$ curve drops towards 0 [Figs. 9(g)–9(i)]. Note that for $\alpha = 1$, $c_g$ is simply the binding rate of the transcriptional repressor to the sRNA promoter. For $\alpha > 1$, it represents the overall rate of a more complicated process, which includes the assembly of a repressor complex of $\alpha$ repressors, and its binding to the promoter site.


[1] G. Storz, S. Altuvia, and K. M. Wasserman, Annu. Rev. Biochem. **74**, 199 (2005).

[2] S. Gottesman, Trends Genet. **21**, 399 (2005).

[3] R. Hershberg, S. Altuvia, and H. Margalit, Nucleic Acids Res. **31**, 1813 (2003).

[4] T. K. E. Levine, Z. Zhang, and T. Hwa, PLoS Biol. **5**, e229 (2007).

[5] E. G. S. Altuvia and H. Wagner, Proc. Natl. Acad. Sci. USA **97**, 9824 (2000).

[6] S. Gottesman and G. Storz, Cold Spring Harbor Perspect. Biol. **3**, 1 (2011).

[7] C. Baker, T. Jia, and R. V. Kulkarni, Phys. Rev. E **85**, 061915 (2012).

[8] Y. Shimoni, G. Friedlander, G. Hetzroni, G. Niv, S. Altuvia, O. Biham, and H. Margalit, Mol. Syst. Biol. **3**, 138 (2007).

[9] P. Mehta, S. Goyal, and N. S. Wingreen, Mol. Syst. Biol. **4**, 221 (2008).

[10] M. Nitzan, P. Fechter, A. Peer, Y. Altuvia, D. Bronesky, F. Vandenesch, P. Romby, O. Biham, and H. Margalit, Nucleic Acids Res. **43**, 1357 (2015).

[11] R. Milo, S. Shen-Orr, S. Itzkovitz, N. Kashtan, D. Chklovskii, and U. Alon, Science **298**, 824 (2002).

[12] S. S. Shen-Orr, R. Milo, S. Mangan, and U. Alon, Nat. Genet. **31**, 64 (2002).

[13] E. Yeger-Lotem and H. Margalit, Nucleic Acids Res. **31**, 6053 (2003).

[14] E. Yeger-Lotem, S. Sattath, N. Kashtan, S. Itzkovitz, R. Milo, R. Y. Pinter, U. Alon, and H. Margalit, Proc. Natl. Acad. Sci. USA **101**, 5934 (2004).

[15] L. V. Zhang, O. D. King, S. L. Wong, D. S. Goldberg, A. H. Tong, G. Lesage, B. Andrews, H. Bussey, C. Boone, and F. P. Roth, J. Biol. **4**, 6 (2005).

[16] P. Mandin and M. Guillier, Curr. Opin. Microbiol. **16**, 125 (2013).

[17] M. Ptashne, *A Genetic Switch: Phage λ and Higher Organisms*, 2nd ed. (Cell Press and Blackwell Scientific Publications, Cambridge, MA, 1992).
[18] T. S. Gardner, C. R. Cantor, and J. J. Collins, Nature (London) **403**, 339 (2000).
[19] J. L. Cherry and F. R. Adler, J. Theor. Biol. **203**, 117 (2000).
[20] T. B. Kepler and T. C. Elston, Biophys. J. **81**, 3116 (2001).
[21] P. B. Warren and P. R. ten Wolde, Phys. Rev. Lett. **92**, 128101 (2004).
[22] P. B. Warren and P. R. ten Wolde, J. Phys. Chem. B **109**, 6812 (2005).
[23] A. M. Walczak, M. Sasai, and P. Wolynes, Biophys. J. **88**, 828 (2005).
[24] A. Lipshtat, A. Loinger, N. Q. Balaban, and O. Biham, Phys. Rev. Lett. **96**, 188101 (2006).
[25] A. Loinger, A. Lipshtat, N. Q. Balaban, and O. Biham, Phys. Rev. E **75**, 021904 (2007).
[26] E. Massé, C. K. Vanderpool, and S. Gottesman, J. Bacteriol. **187**, 6962 (2005).
[27] E. Massé, H. Salvail, G. Desnoyers, and M. Arguin, Curr. Opin. Microbiol. **10**, 140 (2007).
[28] B. Vecerek, I. Moll, and U. Blasi, EMBO J. **26**, 965 (2007).
[29] E. Holmqvist, C. Unoson, J. Reimegard, and E. G. H. Wagner, Mol. Microbiol. **84**, 414 (2012).
[30] F. Fazi, A. Rosa, A. Fatica, V. Gelmetti, M. L. D. Marchis, C. Nervi, and I. Bozzoni, Cell **123**, 819 (2005).
[31] S. Fujita, T. Ito, T. Mizutani, S. Minoguchi, N. Yamamichi, K. Sakurai, and H. Iba, J. Mol. Biol. **378**, 492 (2008).
[32] L. Fontana, E. Pelosi, P. Greco, S. Racanicchi, U. Testa, F. Liuzzi, C. M. Croce, E. Brunetti, F. Grignani, and C. Peschle, Nat. Cell Biol. **9**, 775 (2007).
[33] J. Varhese and S. M. Cohen, Genes Dev. **21**, 2277 (2008).
[34] K. C. Tu, C. M. Waters, S. L. Svenningsen, and B. L. Bassler, Mol. Microbiol. **70**, 896 (2008).
[35] R. J. Johnston, S. Chang, J. F. Etchberger, C. O. Ortiz, and O. Hobert, Proc. Natl. Acad. Sci. USA **102**, 12449 (2005).
[36] B. Novak and J. J. Tyson, Nat. Rev. Mol. Cell Biol. **9**, 981 (2008).
[37] P. François and V. Hakim, Phys. Rev. E **72**, 031908 (2005).
[38] D. Liu, X. Chang, Z. Liu, L. Chen, and R. Wang, PloS One **6**, e17029 (2011).
[39] P. Zhou, S. Cai, Z. Liu, and R. Wang, Phys. Rev. E **85**, 041916 (2012).
[40] S. Wang and S. Raghavachari, Phys. Biol. **8**, 055002 (2011).
[41] J. Lloyd-Price and A. S. Ribeiro, Phys. Rev. E **88**, 032714 (2013).
[42] D. T. Gillespie, J. Phys. Chem. **81**, 2340 (1977).
[43] N. Balaban, J. Merrin, R. Chait, L. Kowalik, and S. Leibler, Science **305**, 1622 (2004).
[44] N. Mirouze, Y. Desai, A. Raj, and D. Dubnau, PLoS Genet. **8**, e1002586 (2012).
[45] F. H. Cahn and M. S. Fox, J. Bacteriol. **95**, 867 (1968).
[46] C. Hadden and E. W. Nester, J. Bacteriol. **95**, 876 (1968).
[47] H. Maamar, A. Raj, and D. Dubnau, Science **317**, 526 (2007).
[48] E. Newman and R. Lin, Annu. Rev. Microbiol. **49**, 747 (1995).
[49] B.-K. Cho, C. L. Barrett, E. M. Knight, Y. S. Park, and B. O. Palsson, Proc. Natl. Acad. Sci. USA **105**, 19462 (2008).
[50] W. R. McClure, Proc. Natl. Acad. Sci. USA **77**, 5634 (1980).
[51] I. Golding, J. Paulsson, S. M. Zawilski, and E. C. Cox, Cell **123**, 1025 (2005).
[52] S. Altuvia, D. Weinstein-Fischer, A. Zhang, L. Postow, and G. Storz, Cell **90**, 43 (1997).
[53] M. Nitzan, K. M. Wassarman, O. Biham, and H. Margalit, Biophys. J. **106**, 1205 (2014).
[54] D. Kennell and H. Riezmak, J. Mol. Biol. **114**, 1 (1977).
[55] W. S. P. Henriksson-Peltola and E. Haggard-Ljungquist, Nucleic Acids Res. **35**, 3181 (2007).